The evaluation of the high-resolution forecasts during GIMEX

Jing-Shan Hong

Computer Center, Central Weather Bureau

1. Introduction

Because of the improved computational speed and development of the mesoscale model, the high-resolution (<10 km), local scale, real-time numerical weather prediction for the mesoscale features can now provide plenty of useful information in complex terrain, urban, coastal and spatially inhomogeneous geographical regions. The high-resolution forecasts also show considerable skill in predicting a number of local, orographically driven circulations, including gap winds, foehn-related phenomena, downslope winds, lee waves, and topographic organization of precipitation (Smith et al. 1997). Many of these features are simply not resolved by coarse-resolution models. Currently the real-time high-resolution models are operational at a number of sites (Mass and Kuo 1998). Although the improved forecast skill in revealing the mesoscale features is suggested by the increased model resolution, the more efforts should be addressed to evaluate the performance of the high-resolution model forecasts via the description of the forecast errors and the verification of the quantitative precipitation forecast (QPF).

There are many documents of model performance for individual case studies (e.g., Roebber and Eise 2001) and over an extended period (e.g., Nutter and Manobianco 1999; White et al. 1999). However, only few evaluated study of the performance for high-resolution model over a large number of forecasts is documented. Since the prominent response of the orographically driven circulations is in the near surface layer, it is necessary to further verify the surface forecasts of the high-resolution model. Recently, Hanna and Yang (2001) evaluated the 4-day model performance for the surface wind speed and direction for the Fifth-Generation Pennsylvania State University-National Center for Atmospheric Research Mesoscale Model (MM5; Grell et al. 1994) of 4-km resolution. Their results showed that the typical bias and root-mean-square-error (rmse) of hourly averaged surfaced wind speed was 1.5 m/s and 2.5 m/s for a wide range of wind speed. The bias and rmse of surface wind direction was about –2° and 66°. They suggested that these uncertainties in wind speed and direction were primary due to random turbulent processes that couldn't be simulated by models and to subgrid variations in terrain and land-use. However, the performance of the high-resolution forecasts may vary by regions, and thus the mesoscale forecasts of varying resolution in different areas should be informative.

Case studies had suggested that mesoscale models ran at high resolution could predict the realistic precipitation structure, especially the topographically organized precipitation system (Colle and Mass 1996). However, although the high-resolution forecasts may result in more realistic looking structure, it is necessary to further verify the QPF of the high-resolution models over longer time period. The more understanding to the QPF is not only to better understand the model precipitation bias but also to feedback to identify the weakness of the model precipitation process. Colle et al. (1999) evaluated the 36-h MM5 precipitation forecasts at 36- and 12-km resolution over the Pacific Northwest and compared with the National Center for Environmental Prediction (NCEP) Eta model at 10-km resolution (Eta-10). They found the MM5 simulations need 12-18 h to spin-up the model precipitation because of the cold start process (no hydrometeors at the beginning of the simulation), and the most skillful 6-h forecast period was from 12- to 18-h. The 12-km MM5 generated too much model precipitation along the steep windward slopes and not enough precipitation in the lee of major barriers. Furthermore, Colle et al. (2000) verified the MM5 precipitation forecast during the 1997-99 cool season over the Pacific Northeast and showed that a noticeable improvement in the skill scores as horizontal resolution was increased from 36- to 12-km resolution, however, the skill was restricted to the heavy rainfall as resolution was going from 12- to 4-km.

Taiwan, a subtropical island (22° – 25.5°N) with complex orographic structures in a limited size (about 400 km long and 150 km wide), most of the orography has the elevations extending above 3000 m within distance of 50 km (Fig. 2). Thus, the orographic and land-sea process induced local circulation is dominant over Taiwan Island. The Green Island Mesoscale Experiment (GIMEX) over the southeast Taiwan was conducted in the Mei-Yu season (May and June) of 2001. The proposed scientific objectives of GIMEX was to better

understanding of the mesoscale circulation and the mesoscale convective system associated with the Mei-Yu front to the southeast of Taiwan (Chen 1992; Hsu and Sun 1994), to document the local circulation, including the split flow and lee vortices, induced by Taiwan orography (Kuo and Chen 1990; Yu et al. 1999), and to improve the understanding the structure of the boundary layer and the development of the land/sea breeze and mountain/valley wind. During the period, a real-time numerical weather prediction suite was run to provide high-resolution forecasts at the Taiwan scale*. The MM5 model was run at the horizontal resolution of 5-km twice a day and forced by initial and boundary conditions from the operational models of Central Weather Bureau (CWB) of Taiwan. The purpose of the paper is to evaluate the performance of the surface forecasts of the high-resolution model and to verify the QPF over the Taiwan island within the 2-month period. Since the more details may be revealed as the resolution increase, the spatial distribution of the forecast skill is also discussed. The description of the model configuration and the data used for verification is presented in section 2. The evaluation of the surface variables and QPF is given in section 3 and 4. Finally is the conclusion.

*The detail output is available on the web page: http://hong.cwb.gov.tw/gimex/gimex.htm

2. Model description

The nonhydrostatic version of the PSU-NCAR MM5 was run twice daily (0000 and 1200 UTC) from 1 May through 30 June 2001 at the Central Weather Bureau (CWB) of Taiwan using the Fijitsu VPP500 super-computer with 4 PEs. There were four nested domains as shown in Fig. 1 with the horizontal resolution (dimension) of 135-km (55x36), 45-km (67x55), 15-km (97x91), and 5-km (130x100), respectively. There were 31 unevenly spaced levels in the vertical. The one-way interface was applied to all the nested domains so that the solutions from the fine domain could not feedback to its mother domain. The outermost domain covered most of Asian and West Pacific area in order to better describe the evolution of the Sub-high over Pacific Ocean and avoid the dilution from the boundary problem due to the Tibetan Plateau. Five-minute and 30-s averaged terrain data were analyzed to the 135~15-km and 5-km model grid, respectively. The highest terrain height over Taiwan for the 5-km resolution is about 2944 m. A 30-s vegetation dataset from U.S. Geological Survey (USGS) was used to

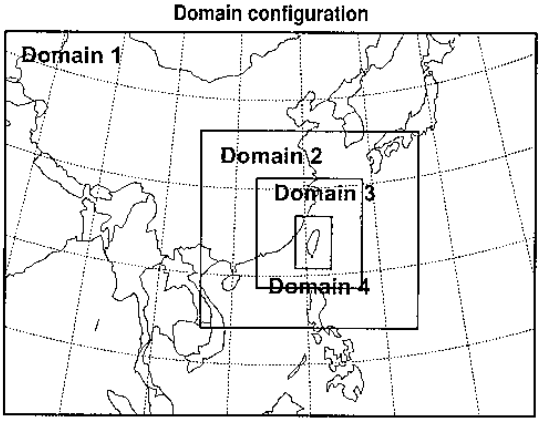

Fig. 1. Computational domains for the four nested grids.

initialize 25 surface categories.

All the MM5 simulation used the explicit moisture scheme of Goddard microphysics (Lin et al. 1983; Tao and Simpson 1993) and the planetary boundary layer parameterization of NCEP's Medium Range Forecast scheme (Hong and Pan 1996). The Kain-Fritsch cumulus parameterization scheme (Kain and Fritsch 1990) was applied in the 135-, 45-, and 15-km domains.

The initial atmospheric conditions and the sea surface temperature were obtained from the operational data assimilation system at CWB, where the analysis package is the Optimal Interpolated scheme (OI) (Barker 1992) at 45-km resolution and then interpolated to all the MM5 domains. The boundary conditions were forced from the forecasts of the operational global model at CWB with update interval of 6-hour. The 48-h forecast for all the MM5 domains was performed during the 2-month period.

3. Data collection and evaluation method

The Central Weather Bureau operates 25 conventional surface stations around Taiwan area. In this study, 18 of the conventional surface stations were selected to evaluate the MM5 surface forecasts. The forecasts of the 5-km-resolution domain were evaluated on 18 stations of 25, which were distributed over Taiwan Island or on the adjacent islands as shown in Fig. 2. The conventional stations were operated in a 3-h interval, most of the stations had the observational interval of 1 hour during the daytime (0800~1700 LST). In the study, the forecasts on the stations were represented by the grid values which the model terrain height were closest to the station height around the station. The reason in stead of using the averaged/weighted method to represent the surface forecast on the station was that the horizontal

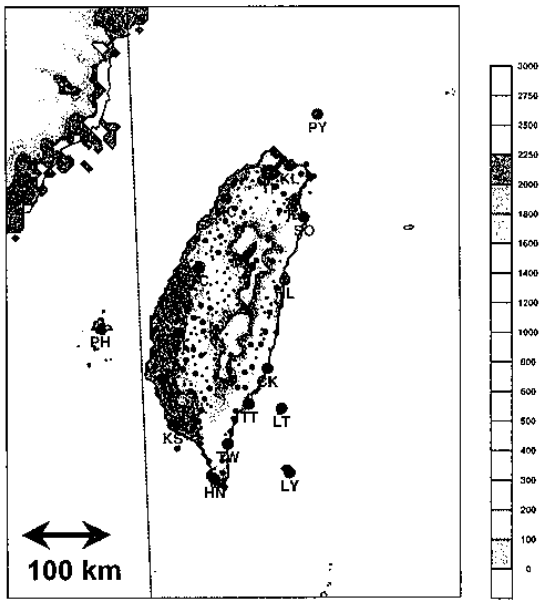

Fig. 2. Topography and the distribution of the conventional surface stations used to evaluate the MM5 surface forecasts (big dots), The rainfall-meteorological stations (middle black dots), and the rainfall stations (small black dots).

Table 1: The comparisons of the station height and the terrain height of the model grids over the station. The last column is the model land-use on the station.

Station ID	Station height	Model terrain	Land/sea
PY	101.7	0.	Sea
KL	26.7	64.9	Land
TP	6.1	0.	Land
IL	7.4	0.	Land
SO	24.9	3.8	Land
HL	16.1	30.5	Land
HC	34.0	36.1	Land
TC	84.0	79.9	Land
CI	26.9	28.1	Land
TN	8.1	12.7	Land
KS	2.3	17.0	Land
PH	10.7	0.8	Land
CK	33.3	214.4	Land
TT	9.0	8.5	Land
TW	8.1	149.0	Land
LY	324.0	33.3	Land
LT	9.0	0.	Sea
HN	22.3	39.3	Land

inhomogeneous may be limited as the model resolution increased, however, the surface forecast error was possible simply attributed by the terrain difference between the model grid and stations, especially over the abrupt orography. The comparisons of the station and model grid parameters were listed on Table 1. Notice that the locations of PY and LT station are on the island which is too small to be described and defined as a sea point in the model. The surface observation from the conventional station were used to verify the model forecasts of the 2-m temperature, 2-m relative humidity, and 10-m wind fields and created the bias (*bias*), root mean square error (*rmse*), and the root mean square vector error (*rmsve*) which were defined as follows:

$$bias = \frac{1}{N}\sum_{i=1}^{N}(O_i - F_i)$$

$$rmse = \sqrt{\frac{1}{N}\sum_{i=1}^{N}(O_i - F_i)^2}$$

$$rmsve = \sqrt{\frac{1}{N}\sum_{i=1}^{N}(u_i^O - u_i^F)^2 + (v_i^O - v_i^F)^2}$$

Where O and F are the observation and forecast, N is the total number of the forecasts. (u, v) is the east- and north-wind component.

In 1982, the CWB initiated a weather hazard prevention program and constructed an Automatic Rainfall and Meteorological Telemetry System (ARMTS). This ARMTS network, completed in August 1997, includes 220 rainfall stations (only observe the precipitation) and 94 rainfall-meteorological stations (observe precipitation, wind, pressure, and temperature). The location of the ARMTS stations is depicted in Fig. 2. The model precipitation of the 5-km-resolution domain was compared to the observed precipitation at each station of the ARMTS network by using the spatial averaging over a grid volume. A number of scores which were computed from the elements of rain/no-rain contingency table (Wilks 1995) including bias score (*Bias*) and equitable threat scores (*ET*). The bias score is defined as

$$Bias = \frac{F}{O},$$

where F is the number of forecasts at the observations with precipitation reach or exceeding a certain threshold amount and O is the number of stations where the observed precipitation meet or exceed the threshold. So the bias score is a way to determine if the model precipitation, averaged over many cases, is overforecast (*Bias*>1) or underforecast (*Bias*<1) for the given threshold and can't provide the accuracy of the forecasts. The equitable threat scores is

defined as (Mesinger 1996)

$$ET = \frac{H - E}{F + O - H - E},$$

$$E = \frac{FO}{N}$$

where H is the number of correctly forecast that both model and observation meet or exceed the given precipitation threshold. F and O are defined above. N is the total number of observations verified.

The model forecasts were collected twice daily (0000 and 1200 UTC) from 0000 UTC 1 May through 1200 UTC 30 June 2001. A total of 109 forecasts out of 122 were verified during the period. The verification procedure was excluded during 0000 UTC 10 May~1200 UTC 13 May and 1200 UTC 21 June to 1200 UTC 23 June, that Taiwan was affected by the landfalling typhoon. During the period, both the surface forecast and QPF tended to have the unreasonable bias due to the inappropriate track forecast. However, accurate prediction of the track and intensity for typhoons affecting Taiwan is not an easy task (Wu and Kuo 1999). The prediction of the typhoon tracks under the influence of the Taiwan orography is a challenging forecast problem and the prediction of the mesoscale features and the precipitation distribution around the island is highly related to the accurate track forecast. In this study, there were no additional typhoon bogusing processes in the initial conditions; thus, the excluding of the 13 forecasts during the typhoon landfalling period would be favor to evaluate the model performance.

4. Verification of surface forecasts

The statistics of the surface forecast errors of the 5-km resolution domain during May and June 2001 were displayed in Table 2. Because of the complexity of the orography over Taiwan and the cold start initiation, in general, the model went through a pronounced adjustment processes during the first few hours, which is most significant in the surface layer. Thus, in order to avoid the unreasonable larger bias due to the adjustment processes, only 7- ~ 48-h forecasts were evaluated to the station observation and were shown in Table 2.

The average of the observed surface temperature was 27.8 °C with higher temperature (>28 °C) over the western plain of Taiwan and lower for the east coastal region. The predicted surface temperature had an averaged warm bias of –0.3 °C and *rmse* of 2.1 °C. The *rmse* was between 1.6 ~ 2.5 °C, in general, the larger bias the larger *rmse*. The further detail analysis found that some systematic temperature biases were occurred for the stations that the differences between the model terrain and station height were large. For example, the location of CK and TW station is at the foothill with large terrain gradient and LY is at the mountaintop of the small island. The limited model terrain had the poor representative for the four stations (see Table 1). As a result, a cold bias on CK and TW stations and large warm bias on LY station were found, where the station height of CK and TW is lower than the model terrain and LY is higher. The empirical correction following the lapse rate might be available to reduce the systematic bias. For example, if we correct the averaged surface temperature forecasts by using the lapse rate of 6.5 °C/km, bias could be modified to about –0.9, –0.7, and 0 °C for LY, CK, and TW station, respectively. The estimated biases accompanied with the bias at TT station made a consistent warm-bias distribution around southeast Taiwan. The diurnal variation was absent on the LT and PY station (not shown), which was due to the incorrect land/sea representative in the model (represented as a sea point as revealed in Table 1). The forecast surface temperature then was closely related to the sea surface temperature. Thus, the more realistic model representative for terrain and land-sea index, especially over the abrupt orography area, is expectable to reduce the systematic surface temperature bias.

One another interested feature was that the surface temperature bias was related to the geographic distribution of the stations. Table 2 showed that most of the cold bias or slight warm bias (e. g. KL, HL, HC, PH, TT, and HN) was occurred for the stations distributed over coastal region. Contrarily, the station located over the inland or the plain area (TP, IL, TC, and TN) had larger warm bias.

The relative humidity displayed in Table 2 showed that the averaged observation is about 78.3% during the evaluated period. The model forecast tended to posses the dry bias of 10%. The *rmse* of relative humidity was about 10~20%. The model also had the bias to predict the stronger wind than observation about 1.3 m/s. The averaged *rmse* for the wind direction and wind speed was about 67.7° and 2.5 m/s, respectively. The averaged *rmsve* for the wind speed was about 3.6 m/s. The larger *rmse* (>3) or *rmsve* (>4) could be found for PY, KL, SO, LT, LY, TW, HN, and KS station, which were distributed over the north- and south-end of Taiwan. Because of the elongated topography as shown in Fig. 2, the most pronounced orographically induced local circulations were occurred over the north/south-end of Taiwan. The features for such an orographically induced local circulation were very sensitive to the up

Table 2: The statistics of the forecast errors for surface temperature, relative humidity and surface winds evaluated on the conventional stations. *Obs*, *bias*, *rmse*, and *rmsve* are the mean of the observations, bias, root mean square error and root mean square vector error, respectively. (detail see the context). The bottom row is the statistics averaged over stations distributed on the Taiwan Island (except PY, PH, LT, and LY station).

Station	Temperature (°C)			Relative humidity (%)			Wind direction (°)			Wind speed (m/s)			
	Obs	*bias*	*rmse*	*Obs*	*bias*	*rmse*	*obs*	*bias*	*rmse*	*obs*	*bias*	*rmse*	*rmsve*
PY	25.6	-0.3	1.9	82.6	7.8	10.3	169.5	19.1	62.1	6.2	0.0	3.2	5.6
KL	27.2	0.9	2.1	75.9	2.5	9.0	115.5	-5.9	70.0	2.5	-1.7	2.7	4.3
TP	28.0	-0.8	2.4	73.5	7.5	12.7	186.3	31.1	75.5	2.4	-0.8	2.1	3.5
IL	26.9	-1.3	2.3	81.8	13.7	16.7	136.4	12.9	71.6	2.0	-1.0	2.1	3.3
SO	26.7	-0.6	1.8	79.5	8.8	12.6	153.7	7.7	75.6	2.5	-1.8	3.0	4.1
HL	27.3	-0.5	1.7	82.1	13.5	16.1	161.8	18.4	74.3	2.9	-0.3	2.2	3.5
HC	27.5	0.5	2.0	75.7	4.0	9.6	175.9	-1.8	57.8	2.5	-1.6	2.8	3.6
TC	28.2	-1.1	2.2	73.3	7.9	12.7	211.7	-9.9	62.1	1.7	-1.0	1.8	2.6
CI	28.2	-0.4	2.0	76.3	7.4	11.9	190.6	-7.6	61.4	2.0	-0.7	2.1	2.9
TN	29.1	-0.9	2.1	79.4	14.7	16.7	208.0	-1.4	64.7	2.6	-0.5	1.8	3.2
KS	28.7	-1.3	2.4	77.9	12.9	16.4	203.3	2.5	68.5	2.2	-1.2	3.1	4.1
PH	28.0	0.5	1.6	83.9	11.4	13.0	157.9	12.1	61.4	2.5	-1.7	2.8	3.6
CK	27.0	0.4	1.7	82.4	10.9	14.1	150.8	17.3	74.2	2.3	-0.6	2.1	3.3
TT	28.1	-0.5	2.1	75.4	7.8	12.0	153.9	18.1	71.8	1.7	-1.7	2.6	3.6
TW	27.6	0.9	2.5	81.5	10.0	15.2	148.3	2.8	66.9	1.9	-2.4	3.3	4.4
LY	25.5	-2.8	3.1	91.8	19.9	20.6	160.2	26.0	67.8	7.9	3.4	5.4	7.3
LT	26.0	-1.6	2.5	89.8	17.8	18.8	105.0	5.3	70.9	3.8	-2.0	4.1	6.1
HN	28.6	0.2	2.0	79.1	8.5	12.6	160.8	14.7	59.7	2.8	-2.1	3.0	4.1
Average	27.8	-0.3	2.1	78.3	9.3	13.5	169.1	7.2	67.7	2.3	-1.3	2.5	3.6

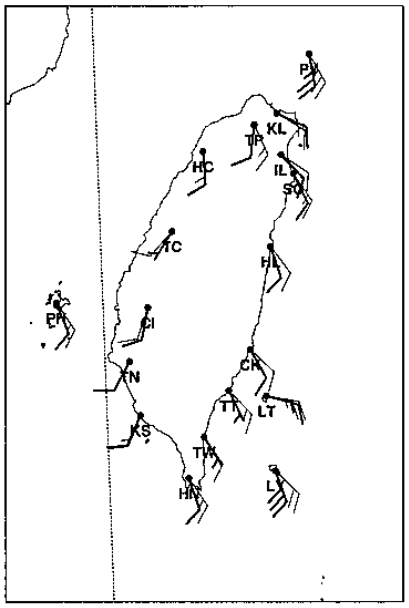

Fig. 3. The averaged surface wind bar for the observations (heave bar) and the forecasts (thin bar) during May and June 2001. The full bar is 5 m/s.

stream condition, which highly relied on the accurate prescription of synoptic system. If the synoptic forecasts have slight temporal or spatial phase error, the high-resolution forecasts might produce large verification errors. Unfortunately, most of the upstream information around Taiwan was over the ocean and absent the enough observations. Thus, the large variability for the forecast errors of the wind speed occurred over the south-/north-end of Taiwan might be, of cause, due to the systematic bias of MM5 or the inaccurate description of the synoptic pattern in the initial condition or the forecasts.

Fig. 3 is the observed and forecast winds averaged over the 2-month period. The figure showed that the averaged wind field during May and June was dominated by the prevailed south wind component and modified by the sea breeze over Taiwan Island. The figure showed that the model forecast wind speed was not only stronger than the observation but also had the direction bias that contained more onshore wind component. The results implied that the model tended to predict stronger sea breeze circulation around Taiwan Island. The influence of the stronger predicted sea breeze could reduce the radiation heating effect and then led to the cold or slight warm bias for the stations distributed along the coastal region.

Fig. 4 was the statistics averaged over stations distributed on Taiwan Island and displayed as function of the forecast time. Only forecasts of the initial at 12Z were used in order to enhance the results of the diurnal cycle. The

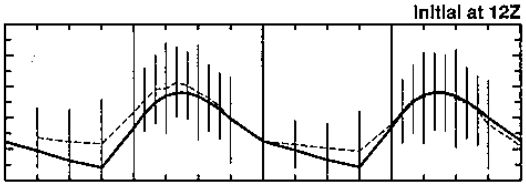

Fig. 4. The statistics for (a) surface temperature, (b) surface relative humidity, and (c) surface wind speed, which averaged over stations distributed on Taiwan Island (except PY, PH, LT, and LY station) during May and June 2001. Results were the initials at 12Z and plotted as function of forecast time (00~48 hour) and the valid local time. The heavy line is the observations and the thin line is the forecasts. The vertical line is the root mean square error of the forecast errors. The model forecasts were verified on the observation time with the 1-h interval during daytime and 3-h during nighttime.

results from the initial at 00Z were similar to Fig. 4 (not shown). The statistics for the surface temperature, relative humidity and wind speed shown in Fig. 4 exhibited the significant diurnal variations: bias and *rmse* during nighttime were larger than that during daytime. Figure 4a also showed that the warm bias was occurred during nighttime whereas the slight cold bias could be found during afternoon that was the period the sea breeze was well developed. The feature further supported the former postulation that the cold bias along the stations distributed over coastal region was due to the reduced radiation heating effect resulted from the over-predicted sea breeze circulation.

The bias and equitable thread scores (*ET* score) for the 5-km resolution domain based on the contingency table were computed at 12-h interval between forecast hour 0~48. Fig. 5 was the bias scores as a function of the rain threshold. The figure showed that the bias scores were less then one for all the rain thresholds and forecast periods. The under-prediction of the precipitation was consistent with the dry bias as depicted in Table 2. The scores decreased 0.15~0.2 from the 0.1 to 1 mm threshold and were almost constant for the other rain threshold. The figure also showed that the bias

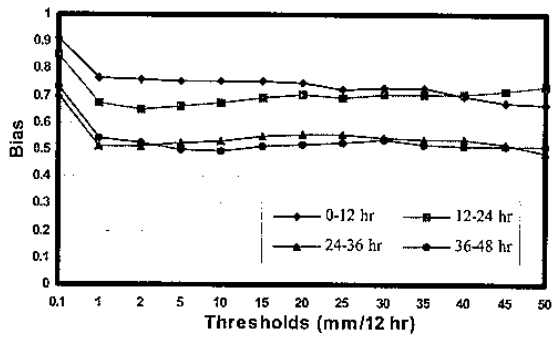

Fig. 5. Bias scores as a function of rain threshold in 12-h interval (0~12-h, 12~24-h, 24~36-h, and 36~48-h forecasts).

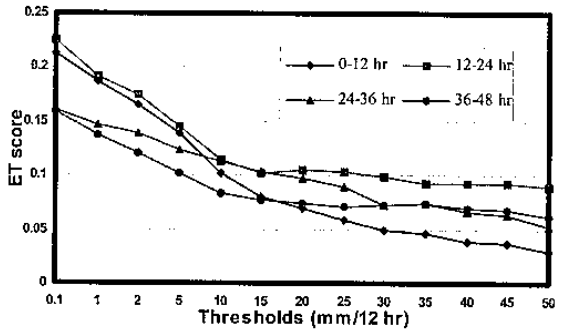

Fig. 6. Same as Fig. 5, but for the equitable threat scores.

at all thresholds decreased as the increasing forecast time. The 24~36-h and 36~48-h forecasts were the modest under-prediction period with the bias scores of 0.5~0.55.

Fig. 6 showed that the most skillful 12-h forecast period during the 48-h forecasts was 12~24-h with *ET* scores from approximately 0.23 to 0.09 for the increasing rain threshold, whereas the worst was the 0~12-h forecast period deceased from 0.22 to 0.03. The *ET* scores for 24~36-h forecast period ranged from 0.16 to 0.05 and was comparable to the 12~24-h forecast period for the 10~20 mm threshold. The under-prediction of the precipitation and poor *ET* scores were possible due to the inadequate prescription of the humidity in the initial condition and the cold-start initialization procedure, which might not well reveal the detail initial mesoscale moisture features. Thus, to improve the initial condition or develop the data assimilation technique for the high-resolution model becomes an important issue.

Summary

The performance of the 5-km resolution MM5 forecast was evaluated during May and June 2001. In overall, the model had an averaged surface warm bias of –0.3 °C and *rmse* of 2.1 °C. The larger biases of the surface temperature were occurred where the difference of the model terrain and station height is large. The stations located around the coastal region had slighter warm bias or cold bias, accompanied with the inland wind bias, implied that the model over-forecasted the sea breeze and then reduced the radiation heating effect. The reduced radiation heating effect might lead to the cold bias of the stations located around coastal region. The forecast relative humidity was 10% drier than observations. The model had the bias to predict the stronger wind than observation about 1.3 m/s. The averaged *rmse* for the wind direction and wind speed was about 67.7° and 2.5 m/s, respectively. The averaged *rmsve* for the wind speed was about 3.6 m/s.

The larger *rmse* for the surface wind speed was found at stations distributed over the north- and south-end of Taiwan. Because of the elongated topography as shown in Fig. 2, the most pronounced orographically induced local circulations were occurred over the north-/south-end of Taiwan. The large variability for the forecast errors of the wind speed occurred over the south-/north-end of Taiwan might be, of cause, due to the systematic bias of MM5 or the inaccurate description of the synoptic pattern in the initial condition or the forecasts.

The statistics for the forecast errors exhibited the significant diurnal variations; the bias and *rmse* during nighttime were larger than that during daytime. The warm bias was occurred during nighttime whereas the slight cold bias could be found during afternoon.

The bias and equitable thread scores (*ET* score) were computed at 12-h interval between forecast hour 0~48. The bias scores were less then one for all the rain thresholds and decreased as the increasing forecast time. The under-prediction of the precipitation was consistent with the dry bias for the surface relative humidity. 12~24-h was the most skillful 12-h forecast period with *ET* scores from approximately 0.23 to 0.09, whereas the worst was the 0~12-h forecast period deceased from 0.22 to 0.03. The under-prediction of the precipitation and poor *ET* scores were possible due to the inadequate prescription of the humidity in the initial condition and the cold-start initialization procedure. Thus, to improve the initial condition or develop the data assimilation technique for the high-resolution model becomes an important issue.

Reference

Baker, E. H., 1992: Design of the navy's multivariate optimal interpolation analysis system. *Wea. Forecasting,* **7**, 220 - 231.

Chen, Y. L., 1992: Some synoptic-scale aspects

of surface fronts over southern China during TAMEX. *Mon. Wea. Rev.*, **121,** 50 –64.

Colle, B. A., and C. F. Mass, 1996: An observational and modeling study of the interaction of low level southwesterly flow with the Olympic Mountains during COAST IOP4. *Mon. Wea. Rev.*, **124,** 2152 - 2175.

Colle, B. A., K. J. Westrick, and C. F. Mass, 1999: Evaluation of MM5 and Eta-10 precipitation forecasts over the Pacific northwest during the cool season. *Wea. Forecasting,* **14,** 137 - 154.

Colle, B. A., C. F. Mass, and K. J. Westrick, 2000: MM5 precipitation verification over Pacific Northeast during the 1997-99 cool season. *Wea. Forecasting,* **15,** 730 - 744.

Cox, R., B. L. Bauer, and T. Smith, 1998: A mesoscale model intercomparison. *Bull. Amer. Metor. Soc.*, **79,** 265 – 283.

Grell, G. A., J. Dudhia, and D. R. Stauffer, 1994: A Description of the Fifth Generation Penn State/NCAR Mesoscale Model (MM5). NCAR/TN-398+1A, National Center for Atmospheric Research, Boulder, CO, 107pp.

Hann, S. R., and R. Yang, 2001: Evaluation of mesoscale models' simulations of near-surface winds, temperature gradients, and mixing depths. *J. Appl. Meteor.*, **40,** 1095 – 1104.

Hong, S. Y., and H. L. Pan, 1996: Nonlocal boundary layer vertical diffusion in a medium-range forecast model. *Mon. Wea. Rev.*, **124,** 2322 - 2339.

Hsu, W. R., and W. Y. Sun, 1994: A numerical study of low level jet and its accompanying second circulation in a Mei-Yu system. Mon. *Wea. Rev.*, **122,** 324 – 340.

Kuo, Y. H., and G. T. J. Chen, 1990: The Taiwan area mesoscale experiment (TAMEX): An overview. *Bull. Amer. Metor. Soc.*, **71,** 488 - 503.

Kain, J. S., and J. M. Fritsch, 1990: A one-dimensional entraining/detraining plume model and its application in convective parameterization. *J. Atmos. Sci,* **47,** 2784 – 2802.

Lin, Y.-L., R. D. Farley, and H. D. Orville, 1983: Bulk parameterization of the snow field in a cloud model. *J. Clim. Appl. Meteor.*, **22,** 1065 - 1092.

Mass, C. F., and Y. H. Kuo, 1998: Regional real-time numerical weather prediction: current status and future potential. *Bull. Amer. Metor. Soc.*, **79,** 253 - 263.

Mesinger, F., 1996: Improvements in quantitative precipitation forecasts with the Eta regional model at the National Centers for Environmental Prediction: The 48-km upgrade. *Bull. Amer. Metor. Soc.*, **77,** 2637 – 2649.

Nutter, P. A., and J. Manobianco, 1999: Evaluation of the 29-km Eta model. Part I: Objective verification at three selected stations. *Wea. Forecasting,* **14,** 5 – 17.

Roebber, P. J., and J. Eise, 2001: The 21 June 1997 Flood: Storm-scale simulations and implications for operational forecasting. *Wea. Forecasting,* **16,** 197 – 218.

Smith, R., and Coauthors, 1997: Local and remote effect of mountains on weather: Research needs and opportunities. *Bull. Amer. Metor. Soc.*, **78,** 877 – 892.

Tao, W.-K., and J. Simpson, 1993: Goddard Cumulus Ensemble Model. Part I: Model Description. *T. A. O.*, **4,** 35 –72.

Terrestrial, Atmospheric and Oceanic Sciences, 4, 35?2.

White, B. G., and Coauthors, 1999: Short-term forecast validation of six models. *Wea. Forecasting,* **14,** 84 - 108.

Wilks, D., 1995: *Statistical Methods in the Atmospheric Sciences: An Introduction.* Academic Press, 467 pp.

Wu, C. C., and Y. H. Kuo, 1999: Typhoons affecting Taiwan: current understanding and future challenges. *Bull. Amer. Metor. Soc.*, **80,** 67 – 80.

Yu, C. K., B. J. D. Jou, and B. F. Smull, 1999: Formative stage of a long-lived mesoscale vortex observed by airborne Doppler radar. *Mon. Wea. Rev.*, **127,** 838 – 857.